

Constraints on the Physical Parameters of the Dark Energy Using A Model-Independent Approach

Ruth A. Daly*

*Department of Physics, Pennsylvania State University,
Berks Campus, Reading, PA 19610*

S. G. Djorgovski†

*Division of Physics, Mathematics, and Astronomy,
California Institute of Technology,
MS 105-24, Pasadena, CA 91125*

(Dated: December 21, 2005)

Understanding the physical nature of the dark energy which appears to drive the accelerated expansion of the universe is one of the key problems in physics and cosmology today. This important problem is best studied using a variety of mutually complementary approaches. Daly and Djorgovski (2003, 2004) proposed a model independent approach to determine a number of important physical parameters of the dark energy as functions of redshift directly from the data. Here, we expand this method to include the determinations of its potential and kinetic energy as functions of redshift. We show that the dark energy potential and kinetic energy may be written as combinations of the first and second derivatives of the coordinate distance with respect to redshift. We expand the data set to include new supernova measurements, and now use a total of 248 coordinate distances that span the redshift range from zero to 1.79. First and second derivatives of the coordinate distance are obtained as functions of redshift, and these are combined to determine the potential and kinetic energy of the dark energy as functions of redshift. An update on the redshift behavior of the dimensionless expansion rate $E(z)$, the acceleration rate $q(z)$, and the dark energy pressure $p(z)$, energy density $f(z)$, and equation of state $w(z)$ is also presented. We find that the standard $\Omega_{0m} = 0.3$ and $\Omega_{\Lambda} = 0.7$ model is in an excellent agreement with the data. We also show tentative evidence that the Cardassian and Chaplygin gas models in a spatially flat universe do not fit the data as well.

I. INTRODUCTION

The acceleration of the universe at the present epoch can be studied using a variety of techniques such as type Ia supernovae [1, 2, 3, 4, 5, 6, 7], and studies of cosmic microwave background radiation (e.g., [8]) combined with large scale structure studies (e.g. [9, 10]), which indicate that at the present epoch the universe is expanding at an accelerating rate. Studies of powerful FRII radio galaxies also indicate that the universe is accelerating [11, 12, 13]. To study this in detail, it is important to determine the redshift behavior of the expansion and acceleration rates of the universe, and the properties and redshift evolution of the driver(s) of these rates.

In this vein, [14, 15] suggest a model-independent method of studying the redshift evolution of the expansion and acceleration rates of the universe, and show that the acceleration of the universe can be written in terms of the first and second derivatives of the coordinate distance with respect to redshift. These derivatives are obtained directly from the data on coordinate distances using a statistically robust numerical technique. The accelera-

tion thus derived requires very few assumptions, relying only upon the assumptions that the universe is homogeneous and isotropic on large scales, and has zero space curvature. Indeed, this approach allows a determination of the acceleration of the universe that is independent of a theory of gravity and of the properties and redshift evolution of the drivers of the expansion and acceleration, such as dark energy, dark matter, or other components. Complementary model-independent approaches based on an integral rather than a differential technique are discussed by [16, 17, 18, 19, 20, 21, 22, 23].

Understanding the properties of the physical driver of the acceleration of the universe is of fundamental importance. The driver, commonly referred to as the dark energy, and its properties are parameterized in quantities such as the potential and kinetic energy, and the pressure, energy density, and equation of state. These quantities can be expressed as combinations of the first and second derivative of the coordinate distance, as discussed by [15].

Here, we show that the dark energy potential and kinetic energy may be determined as functions of redshift by appropriately combining the first and second derivatives of the coordinate distance to sources at different redshift. This expansion of the method is described in section II. The method is applied to an enlarged data sample which includes the 71 new Legacy supernovae coordinate distances, presented in section III, and the co-

*Electronic address: rdaly@psu.edu

†Electronic address: george@astro.caltech.edu

ordinate distances listed in [15].

The work presented here on the dark energy potential, $V(z)$, and kinetic, $K(z)$, energy is complementary to the work of [18], [24] and [25]. Saini et al. [18] derive equations for $V(z)$ and $K(z)$ and use a fitting function for the luminosity distance to obtain values and uncertainties for the parameters of the fitting function; these are then used to obtain $V(z)$, $K(z)$, and the equation of state parameter $w(z)$. Simon et al. [24] consider the reconstruction of the dark energy potential based on an expansion of the dark energy potential in terms of Chebyshev polynomials, while [25] consider the expansion of the quintessence potential V as a power series of the quintessence field ϕ . [18], [24] and [25] find that the results are consistent with those expected if a cosmological constant is driving the acceleration of the universe at the present epoch.

II. THE POTENTIAL AND KINETIC ENERGY OF THE DARK ENERGY

The potential and kinetic energy of the dark energy can be determined as functions of redshift using measurements of the coordinate distance. Measurements of the coordinate distance obtained using type Ia supernovae and type IIb radio galaxies allow determinations of the first and second derivative of the coordinate distance with respect to redshift. For detailed discussion of numerical methods used to derived these quantities as well as extensive tests of the methods, see [14, 15]. These derivatives may be combined to obtain $V(z)$ and $K(z)$, the potential and kinetic energy density of the dark energy, which, for convenience, are expressed in units of the critical density at the current epoch.

It is well known that $V = 0.5(\rho - P)$ and $K = 0.5(\rho + P)$, where ρ and P are the energy density and pressure of the dark energy. In [15] we show that both ρ and P may be written in terms of the first and second derivatives of the coordinate distance (see Eqs. [6] and [7] of [15]). Combining these, we find that

$$\left(\frac{V}{\rho_{oc}}\right) = (y')^{-2} [1 + (1+z)(y'')(y')^{-1}/3] - 0.5\Omega_{0m}(1+z)^3 \quad (1)$$

and

$$\left(\frac{K}{\rho_{oc}}\right) = -(1/3)(1+z)(y'')(y')^{-3} - 0.5\Omega_{0m}(1+z)^3, \quad (2)$$

where ρ_{oc} is the critical density at the current epoch, the dimensionless coordinate distance $y(z) \equiv H_0(a_0r)$, H_0 is Hubble's constant, (a_0r) is the coordinate distance to a source at redshift z , $y' \equiv (dy/dz)$, and $y'' \equiv (d^2y/dz^2)$.

In obtaining Eqs. [1] and [2], it has been assumed that: the universe is spatially flat; the kinematics of the universe are accurately described by general relativity; and two components, the dark energy and non-relativistic matter, are sufficient to account for the kinematics of the

universe out to redshift of about 2 (see the discussion in [15]).

Thus, the redshift behavior of the potential and kinetic energy densities of the dark energy can be constructed using the first and second derivatives of the dimensionless coordinate distance $y(z)$, for the data set described below.

III. THE DATA SET

The core of our data set remains the sample of 157 "Gold" supernovae of [6] and the 20 radio galaxids of [11], both of which are tabulated in [15]. This data set is supplemented by 71 new supernovae from the Supernova Legacy Survey of [7], which allows the determination of dimensionless coordinate distances to 71 additional type Ia supernovae. These are listed in Table I, and were obtained using the values and uncertainties of μ_B listed in Table 9 of [7], given the value of $H_0 = 70$ km/s/Mpc adopted by [7]. Two uncertainties of y are listed: $\sigma(y)$ is obtained from the uncertainty in μ_B listed in Table 9 of [7], while the total uncertainty of y (used throughout this paper) $\sigma_T(y)$ reflects the total uncertainty of μ_B , which is obtained by adding in quadrature the uncertainty listed in Table 9 to the intrinsic dispersion of 0.13 identified by [7]. These are listed in Table I.

The total sample of 248 sources, including 228 supernovae and 20 radio galaxies, is shown in Fig. 1. We note that there are no systematic differences seen among the three groups of measurements in the redshift ranges of their overlaps.

IV. RESULTS OBTAINED WITH THE FULL SAMPLE OF 248 SOURCES

Values of y' and y'' obtained with the full sample are shown in Figs. [2], and [4]. As in [14, 15], a window function with Δz of 0.6 is used in this paper. Note that the first and second derivatives are obtained directly from the measured values of y ; no assumptions have been adopted regarding a theory of gravity, or the form of the expansion or acceleration rate of the universe as a function of redshift. For comparison, the values of parameters predicted in a standard lambda cold dark matter (LCDM) cosmological model, where the kinematics of the universe are described by general relativity and the primary components of the universe at present are a normalized cosmological constant $\Omega_\Lambda = 0.7$ and non-relativistic matter $\Omega_{0m} = 0.3$, are shown on each figure. In addition, the curve expected in a universe with space curvature k is shown in Fig. [2], where values of $\Omega_{0m} = 0.3$, $\Omega_\Lambda = 0$, and $\Omega_R = -k/(a_0H_0)^2 = 0.7$ have been assumed. Clearly, this curvature dominated model is inconsistent with the results obtained here.

To compare our results with those expected in a LCDM model a mock data set of 248 sources was constructed in

TABLE I: Coordinate distances to the 71 Legacy Supernovae and their uncertainties.

name	z	y	σ (y)	σ_T (y)
SNLS-03D1au	0.504	0.475	0.0085	0.0297
SNLS-03D1aw	0.582	0.556	0.0138	0.0360
SNLS-03D1ax	0.496	0.426	0.0074	0.0265
SNLS-03D1bp	0.346	0.325	0.0031	0.0197
SNLS-03D1cm	0.870	0.822	0.1140	0.1242
SNLS-03D1co	0.679	0.665	0.0269	0.0480
SNLS-03D1ew	0.868	0.743	0.1177	0.1258
SNLS-03D1fc	0.331	0.271	0.0016	0.0163
SNLS-03D1fl	0.688	0.562	0.0127	0.0360
SNLS-03D1fq	0.800	0.647	0.0268	0.0471
SNLS-03D1gt	0.548	0.554	0.0204	0.0389
SNLS-03D3af	0.532	0.502	0.0192	0.0357
SNLS-03D3aw	0.449	0.380	0.0077	0.0240
SNLS-03D3ay	0.371	0.338	0.0047	0.0207
SNLS-03D3ba	0.291	0.286	0.0044	0.0177
SNLS-03D3bh	0.249	0.243	0.0022	0.0147
SNLS-03D3cc	0.463	0.417	0.0065	0.0258
SNLS-03D3cd	0.461	0.407	0.0109	0.0267
SNLS-03D4ag	0.285	0.254	0.0018	0.0153
SNLS-03D4at	0.633	0.605	0.0178	0.0404
SNLS-03D4cn	0.818	0.653	0.0914	0.0994
SNLS-03D4cx	0.949	0.602	0.0754	0.0836
SNLS-03D4cy	0.927	0.986	0.1725	0.1823
SNLS-03D4cz	0.695	0.554	0.0219	0.0398
SNLS-03D4dh	0.627	0.508	0.0082	0.0315
SNLS-03D4di	0.905	0.676	0.0803	0.0899
SNLS-03D4dy	0.604	0.463	0.0062	0.0284
SNLS-03D4fd	0.791	0.610	0.0214	0.0423
SNLS-03D4gf	0.581	0.526	0.0114	0.0335
SNLS-03D4gg	0.592	0.477	0.0198	0.0347
SNLS-03D4gl	0.571	0.462	0.0149	0.0314
SNLS-04D1ag	0.557	0.476	0.0064	0.0292
SNLS-04D1aj	0.721	0.594	0.0290	0.0459
SNLS-04D1ak	0.526	0.517	0.0131	0.0336
SNLS-04D2cf	0.369	0.338	0.0025	0.0204
SNLS-04D2fp	0.415	0.373	0.0046	0.0228
SNLS-04D2fs	0.357	0.334	0.0028	0.0202
SNLS-04D2gb	0.430	0.370	0.0065	0.0231
SNLS-04D2gc	0.521	0.472	0.0117	0.0306
SNLS-04D2gp	0.707	0.607	0.0361	0.0512
SNLS-04D2iu	0.691	0.587	0.0368	0.0509
SNLS-04D2ja	0.741	0.649	0.0350	0.0523
SNLS-04D3co	0.620	0.581	0.0161	0.0383
SNLS-04D3cp	0.830	0.973	0.1556	0.1661
SNLS-04D3cy	0.643	0.571	0.0155	0.0376
SNLS-04D3dd	1.010	0.999	0.2451	0.2523
SNLS-04D3df	0.470	0.451	0.0066	0.0278
SNLS-04D3do	0.610	0.525	0.0094	0.0328
SNLS-04D3ez	0.263	0.253	0.0015	0.0152
SNLS-04D3fk	0.358	0.339	0.0020	0.0204
SNLS-04D3fq	0.730	0.613	0.0212	0.0424
SNLS-04D3gt	0.451	0.411	0.0057	0.0253
SNLS-04D3gx	0.910	0.868	0.1384	0.1478
SNLS-04D3hn	0.552	0.467	0.0075	0.0290
SNLS-04D3is	0.710	0.589	0.0209	0.0410
SNLS-04D3ki	0.930	0.930	0.1841	0.1924
SNLS-04D3kr	0.337	0.312	0.0014	0.0187
SNLS-04D3ks	0.752	0.573	0.0238	0.0418
SNLS-04D3lp	0.983	0.723	0.1650	0.1706

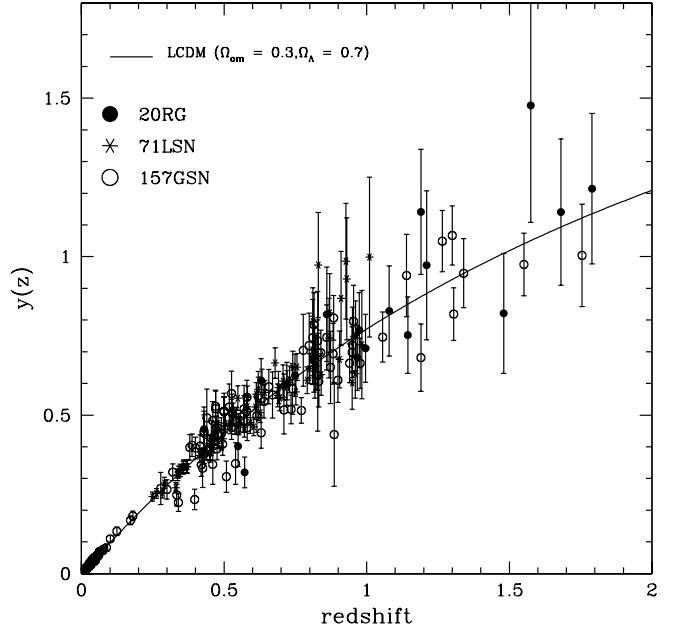


FIG. 1: Coordinate distances to the 71 Legacy and 157 Gold supernovae and 20 radio galaxies.

TABLE II: Table 1 *Continued*

name	z	y	σ (y)	σ_T (y)
SNLS-04D3lu	0.822	0.655	0.0658	0.0766
SNLS-04D3ml	0.950	0.739	0.0912	0.1014
SNLS-04D3nc	0.817	0.690	0.0807	0.0907
SNLS-04D3nh	0.340	0.320	0.0018	0.0193
SNLS-04D3nr	0.960	0.631	0.0680	0.0778
SNLS-04D3ny	0.810	0.706	0.0978	0.1065
SNLS-04D3oe	0.756	0.652	0.0174	0.0427
SNLS-04D4an	0.613	0.566	0.0159	0.0374
SNLS-04D4bk	0.840	0.628	0.0535	0.0654
SNLS-04D4bq	0.550	0.473	0.0122	0.0308
SNLS-04D4dm	0.811	0.794	0.0966	0.1077
SNLS-04D4dw	0.961	0.751	0.1003	0.1099

which the mock sources have the same redshift distribution and fractional error per point as the empirical data but have values of y predicted in a LCDM model with $\Omega_\Lambda = 0.7$ and $\Omega_{0m} = 0.3$. This mock data set was passed through the same numerical programs as the true data, and the results obtained for y' and y'' for both the true and mock data sets are shown in Figs. [3] and [5]. It is quite clear that no bias is introduced by the numerical differentiation; the central value of y' and y'' output by the numerical differentiation lie on those predicted in the assumed LCDM model, and the magnitude of the error bars at a given redshift have the same magnitude as those obtained from the data.

Values of the dimensionless expansion rate $E(z)$, and the deceleration parameter $q(z)$ are shown in Figs. [6]

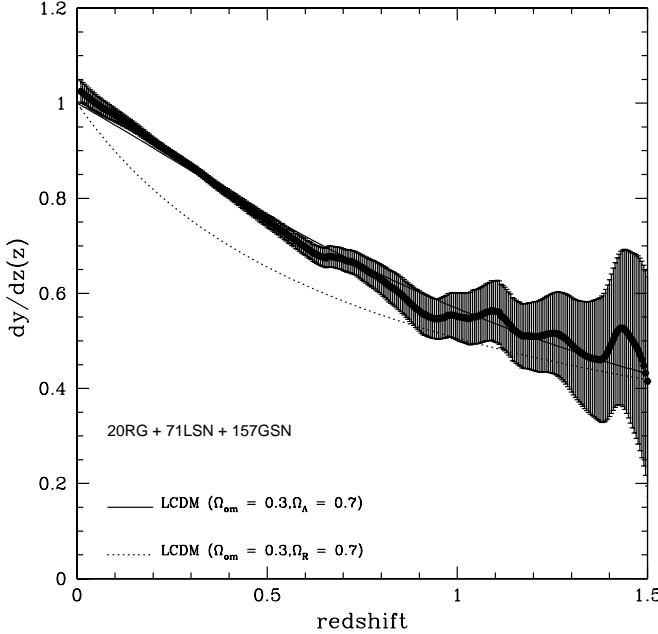


FIG. 2: The first derivative of the coordinate distance with respect to redshift. The values for the standard LCDM model with $\Omega_\Lambda = 0.7$ and $\Omega_{0m} = 0.3$ are shown as the solid line in this and all subsequent plots. The values for the curvature-dominated model described in the text are shown with the dotted line. The zero redshift value we measure is $y'_0 = 1.025 \pm 0.022$. The predicted value is 1.000.

and [9], obtained using equations [5] and [6] of [14]. The only assumptions that must be adopted to construct E and q from y' and y'' are that the universe is homogeneous and isotropic on large scales, and is spatially flat (see [14]). Again, the curve expected in a LCDM model with $\Omega_\Lambda = 0.7$ and $\Omega_{0m} = 0.3$ is shown in each figure. In addition, the curves predicted in two modified gravity models is a spatially flat universe are included in Fig. [6]. These are obtained using the best fit model parameters obtained by [26] for the Cardassian model of [27] and the generalized Chaplygin gas model of [28] based on the model of [29]. Clearly, the LCDM model provides a better description of the data than do either of the modified gravity models.

Fig. [8] shows the difference between values of $E(z)$ and those expected in a LCDM model with $\Omega_\Lambda = 0.7$ and $\Omega_{0m} = 0.3$. This further illustrates how well General Relativity with a cosmological constant describes the data over the very large length scale of greater than about 10 billion light years. Recall that $E(z)$ is derived from the data without having to specify a theory of gravity.

The results shown for $q(z)$ allow a determination of the redshift at which the universe transitions from an accelerating phase to a decelerating phase; we find this to be at a redshift of $z_T = 0.42 \pm 0.08$, consistent with the values quoted by [14, 15] and [6]. The upper bound on

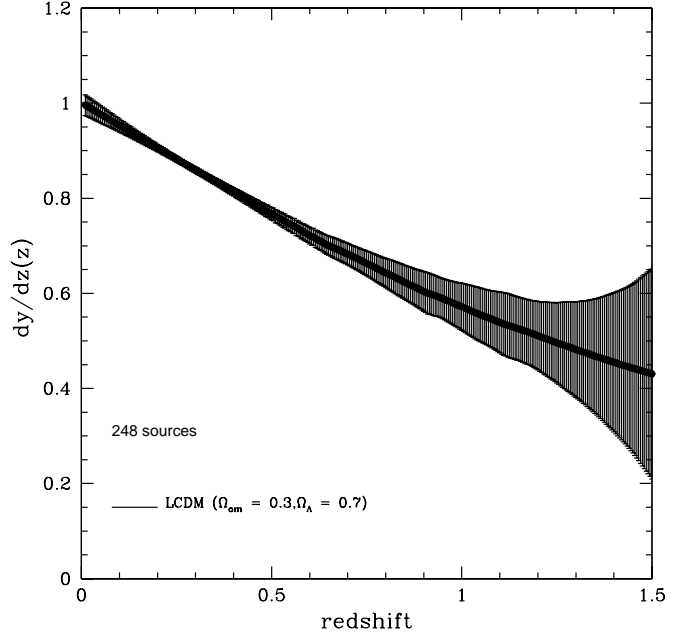


FIG. 3: As in Fig. 2, but for the mock data set with the same redshift and error distribution as the actual data set, with the assumed cosmology with $\Omega_\Lambda = 0.7$ and $\Omega_{0m} = 0.3$. The fit results for this mock data set are in an excellent agreement with the analytical prediction for the assumed cosmology, giving us a confidence that the numerical method we use is unbiased and is capable of recovering accurately the underlying cosmology.

this transition redshift is uncertain because of the fluctuations in $q(z)$ which are due to sparse sampling at high redshift. In this plot, and in the ones that follow, we do not consider these fluctuations at higher redshifts to be statistically significant, as they are commensurate with our derived $1-\sigma$ error bars.

A comparison with these results and those expected in a LCDM model is shown in Figs. [7] and [10], where the predicted values of $E(z)$ and $q(z)$ are obtained using the mock data set described above. Again, we see that no bias has been introduced by the numerical differentiation technique, and the data are in very good agreement with the standard LCDM model.

To obtain the pressure, a theory of gravity must be specified, and general relativity has been assumed here (see eqs. [5] and [6] of [15]). Note that if the dark energy is a cosmological constant, the zero redshift value of $p = P/\rho_{oc}$ is a measure of Ω_Λ . The pressure of the dark energy, in units of the critical density today, obtained with the current data set is shown in Fig. [11]. The zero redshift value suggests $\Omega_\Lambda = 0.61 \pm 0.08$, in excellent agreement with the values commonly derived using more traditional approaches.

Values of $p(z)$ expected in a LCDM model are shown in Fig. [12], where the predicted values of $p(z)$ are obtained using the mock data set described above. Again,

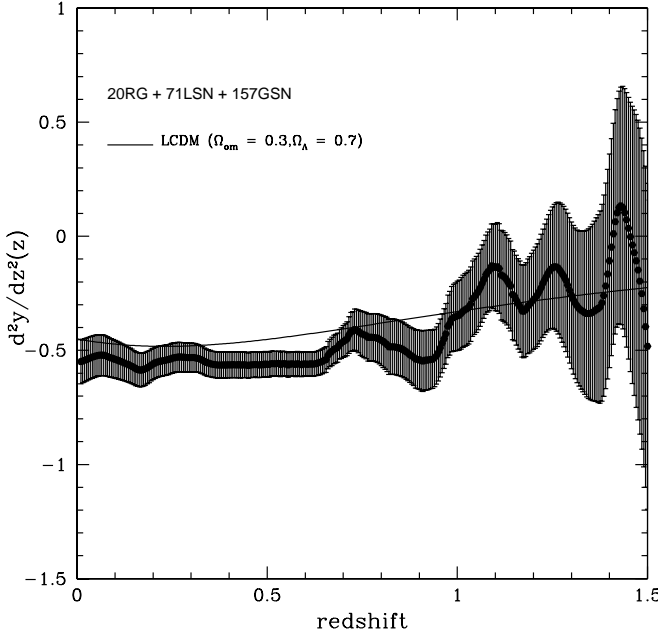


FIG. 4: The second derivative of the coordinate distance with respect to redshift. The measured zero redshift value is $y''_0 = -0.55 \pm 0.10$; the value predicted in a standard LCDM model is -0.45 .

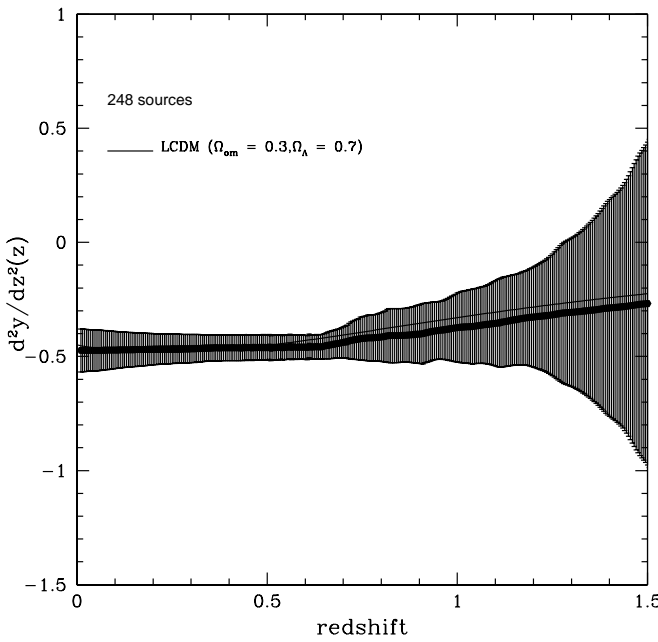


FIG. 5: As in Fig. 4, but for the same mock data set. Again, the correct assumed cosmology is recovered with a negligible bias.

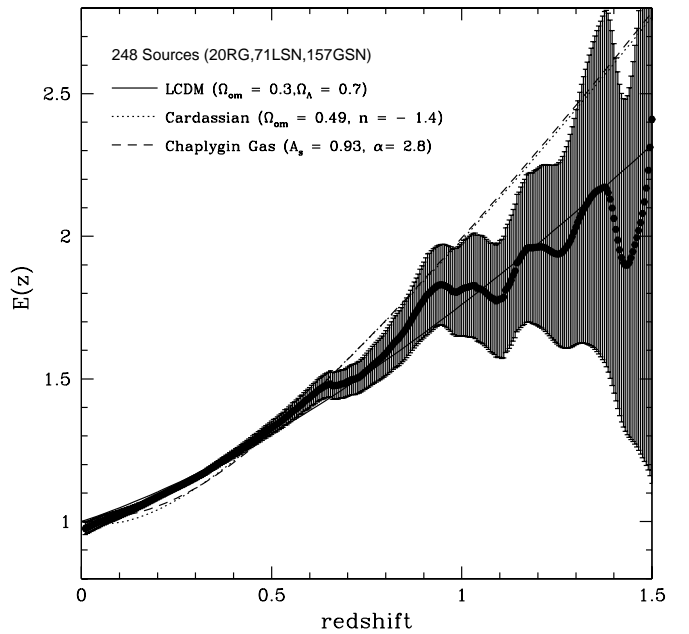


FIG. 6: The dimensionless expansion parameter $E(z)$. The measured zero redshift value is $E_0 = 0.98 \pm 0.02$. The predicted value is 1.00. The solid line shows the prediction of the standard $\Omega_A = 0.7$ and $\Omega_{0m} = 0.3$ model, which is in an excellent agreement with the data. The dotted line represents predictions of the Cardassian model, and the dashed line represents the Chaplygin gas model, obtained assuming that the universe is spatially flat, both of which seem to fit the data systematically less well.

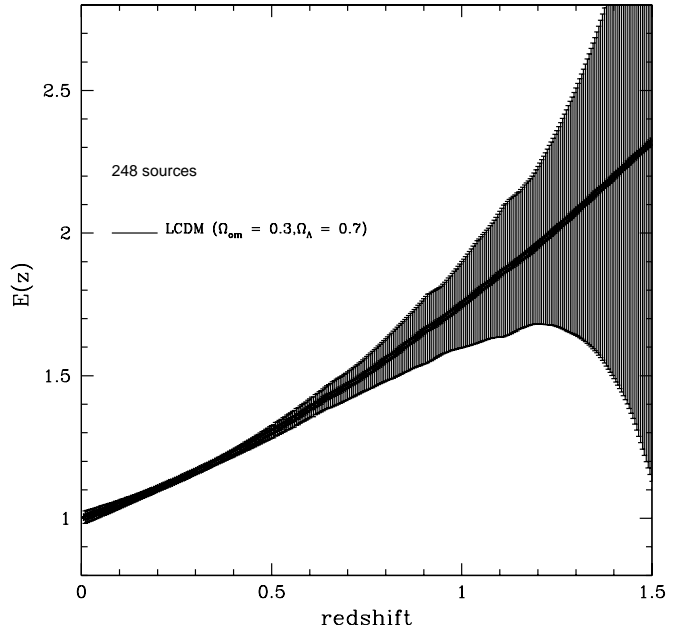


FIG. 7: Derived values of $E(z)$ for the mock data set. Again, the correct cosmology is recovered accurately by the method.

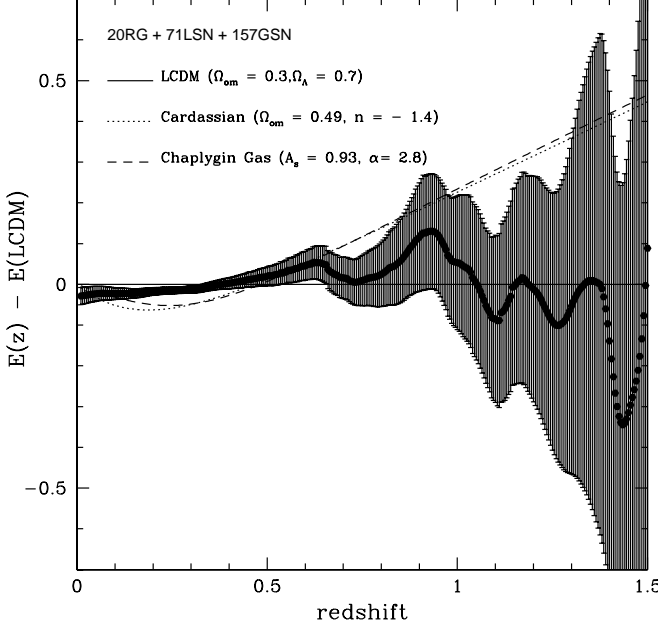


FIG. 8: Values of $E(z)$ relative to the LCDM model with $\Omega_\Lambda = 0.7$ and $\Omega_{0m} = 0.3$, which has been subtracted from the data and the models. This shows how well the LCDM model describes $E(z)$ and that the Cardassian model and generalized Chaplygin gas model in a spatially flat universe seem to fit the data systematically less well.

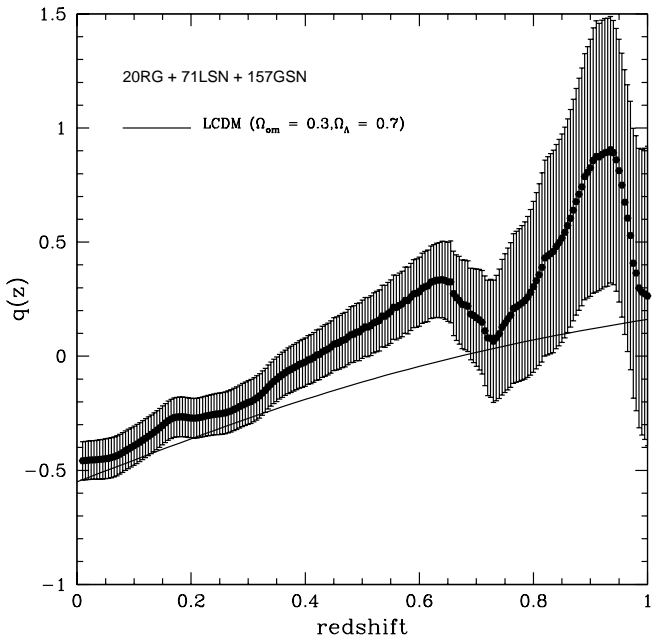


FIG. 9: The deceleration parameter $q(z)$. The zero redshift value is $q_0 = -0.46 \pm 0.08$. The predicted value in a standard LCDM model is -0.55 . Our fits are systematically too high by about 1σ relative to the standard model.

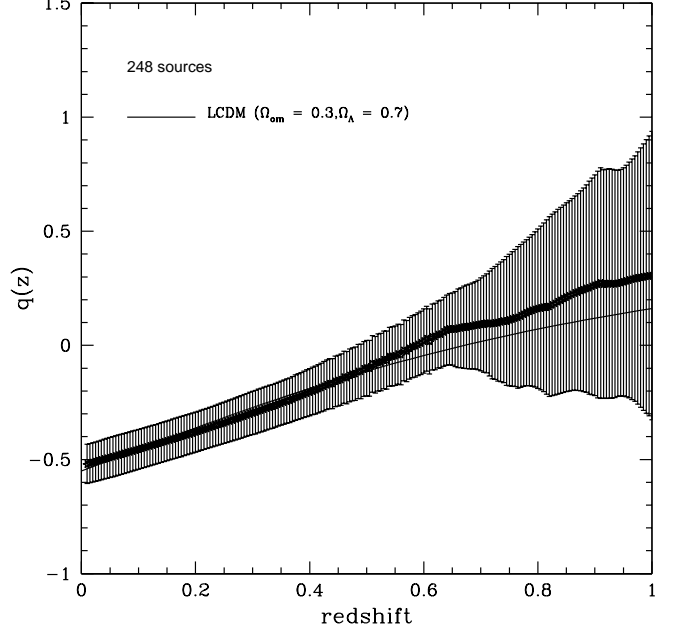


FIG. 10: Derived values of the $q(z)$, but for the mock data set. Again, the underlying cosmology is recovered, except for a slight bias at the high redshift end.

there is no bias introduced by the numerical differentiation technique, and the output is in good agreement with predictions in a LCDM model.

The energy density $f(z) = \rho/\rho_{oc}$ of the dark energy in units of the critical density today can be obtained once a value for Ω_{0m} has been adopted. The value of $f(z)$ obtained assuming $\Omega_{0m} = 0.3$ is shown in Fig. [13]. These results are compared with predictions in a LCDM model obtained with the mock data set in Fig. [14]. There is good agreement between the data and predictions in a LCDM model.

The equation of state of the dark energy, $w = \rho/P$ is shown in Fig. [15]. Results obtained with the mock data set obtained in a LCDM model are shown in Fig. [16]. Figs. [6, 9, 11, 13] and [15] provide an update on the results presented by [15]; the dependence of each quantity on the first and second derivatives of the dimensionless coordinate distance y with respect to redshift z is given in [15].

The values of V and K obtained with the full sample of 248 sources are shown in Figs. [17] and [19]. The results are consistent with a dark energy potential energy that is constant from a redshift of zero to a redshift of about 0.8, as expected if the dark energy is a cosmological constant. The zero redshift normalization depends on $y'(z = 0)$ and $y''(z = 0)$ (see Eq. [1]). The value of y'' at $z=0$ is -0.55 ± 0.1 , while that of y' is 1.03 ± 0.02 ; these cause the value of $V(z=0)$ to be low relative to a LCDM model with $\Omega_{0m} = 0.3$. When the number of low-redshift type Ia supernovae is substantially increased, we expect to be

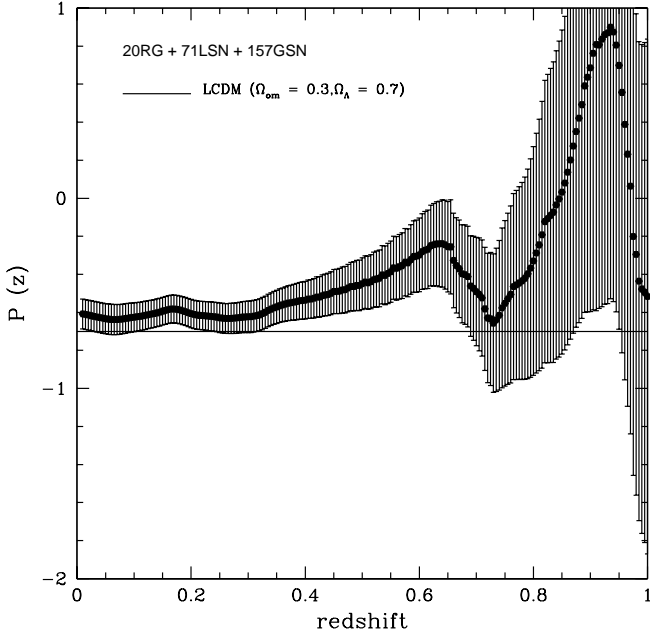


FIG. 11: The pressure of the dark energy in units of the critical density today. The zero redshift value of $p_0 = -0.61 \pm 0.08$.

able to determine whether the normalization of V differs from that expected in a standard LCDM model. These are compared with predictions in a LCDM model using the mock data set, as shown in Figs. [18] and [20]; a LCDM model provides a good description of the data.

We do not understand completely the small systematic difference between our evaluations of some of the observed trends from the standard LCDM model: our values being systematically too high for the $q(z)$, $P(z)$, and $w(z)$, and too low for $V(z)$, by about 1σ throughout. We are inclined to interpret this as the inherent limitation of the current data set, rather than as a real physical effect.

V. SUMMARY AND CONCLUSIONS

The redshift behavior of the potential and kinetic energy of the dark energy can be determined directly from observed quantities without having to assume an a priori functional form for these quantities. They depend upon the first and second derivatives of the coordinate distance with respect to redshift, and on the zero redshift value of the mean mass density in non-relativistic matter. These quantities, y' , y'' , $V(z)$, and $K(z)$ were obtained using a sample of 248 sources including 228 type Ia supernovae and 20 type IIb radio galaxies. In all cases, the results are consistent with predictions of a LCDM model out to a redshift of about one.

The data may also be used to determine the decel-

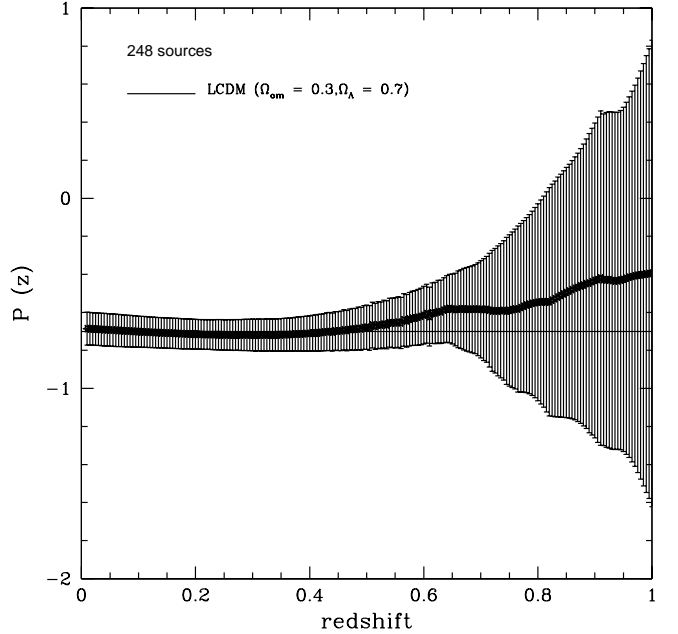


FIG. 12: Values of the $P(z)$, but for the mock data set. The assumed cosmology is recovered accurately.

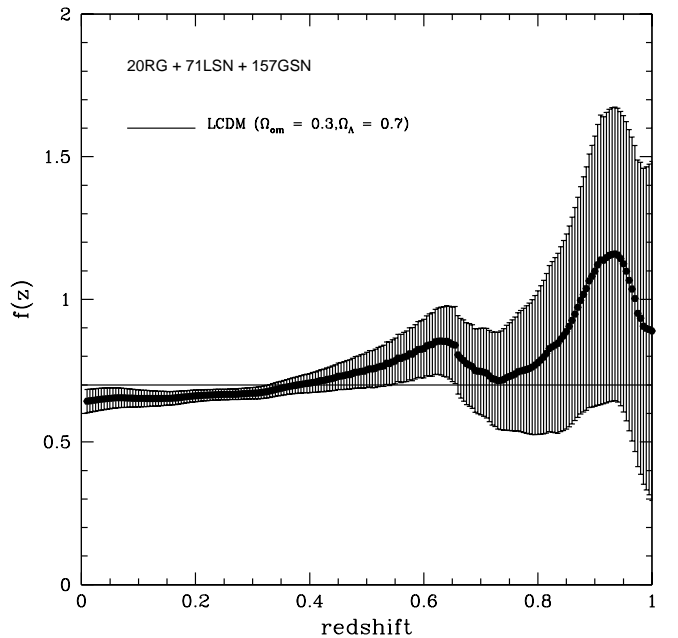


FIG. 13: The energy density of the dark energy in units of the critical density today, $f(z)$. The zero redshift value is $f_0 = 0.64 \pm 0.04$, again in an excellent agreement with the more traditional determinations of Ω_Λ .

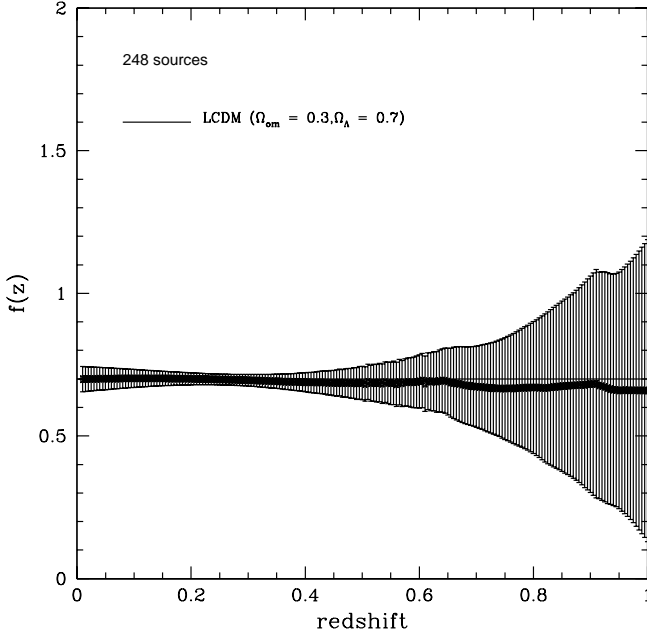


FIG. 14: The values of $f(z)$ for the mock data set. The assumed value of 0.7 is recovered accurately.

eration parameter $q(z)$ and the dimensionless expansion parameter $E(z)$ directly from y' and y'' ; these determinations of q and E assume only that the universe is homogeneous and isotropic on large scales, and is spatially flat, and are independent of any assumptions regarding a theory of gravity or the properties of the dark energy, as discussed in detail by [14, 15]. We find that the universe transitions from an accelerating phase to a decelerating phase at a redshift of $z_T = 0.42 \pm 0.08$. The fact that y , y' , and y'' match predictions in a LCDM model to about one sigma or better to a redshift of about 1.5 means that General Relativity with a cosmological constant provides an accurate description of the data on scales of about 10 billion light years. The correct explanation of the dark energy must be able to account for the observed values of $y(z)$, $y'(z)$ and $y''(z)$, or, equivalently, $y(z)$, $E(z)$, and $q(z)$.

By adopting general relativity as the correct theory of gravity, the pressure of the dark energy can be obtained as a function of redshift. As shown by [15], this depends only upon y' and y'' ; it is independent of assumptions regarding the properties of the dark energy and independent of Ω_{0m} . If the universe is dominated by a cosmological constant at the present epoch, the zero redshift value of p yields a new method of determining Ω_Λ , and the value obtained here is 0.61 ± 0.08 . This is remarkably close to values obtained with more traditional approaches.

The energy density and equation of state of the dark energy may be obtained as functions of redshift if the value of Ω_{0m} is known. These were determined assuming

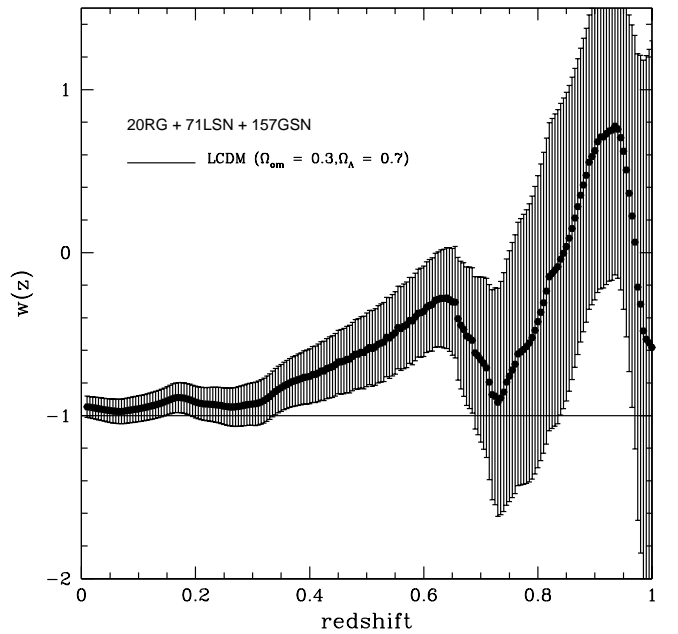


FIG. 15: The dark energy equation of state parameter $w(z)$. The zero redshift value is $w_0 = -0.95 \pm 0.07$, whereas $w = -1$ is the theoretical value for the cosmological constant model.

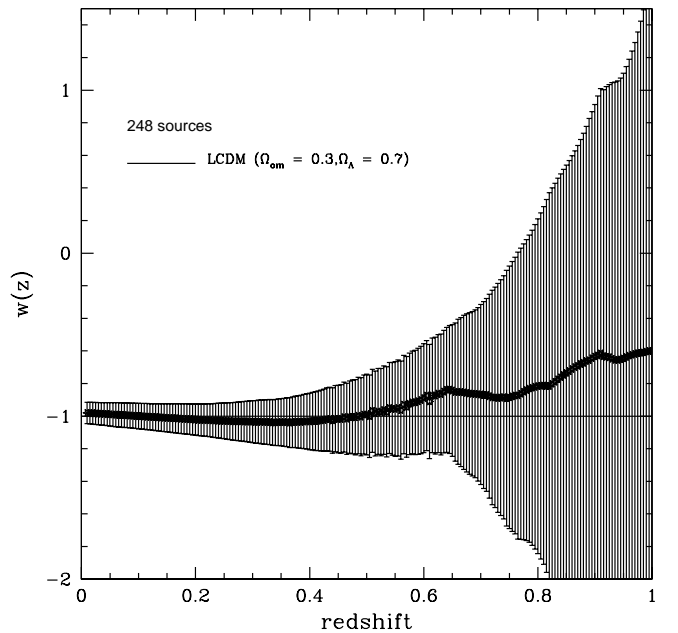


FIG. 16: The values of $w(z)$ for the mock data set. The assumed value of $w = -1$ is recovered accurately, with only a modest bias at the high redshift end.

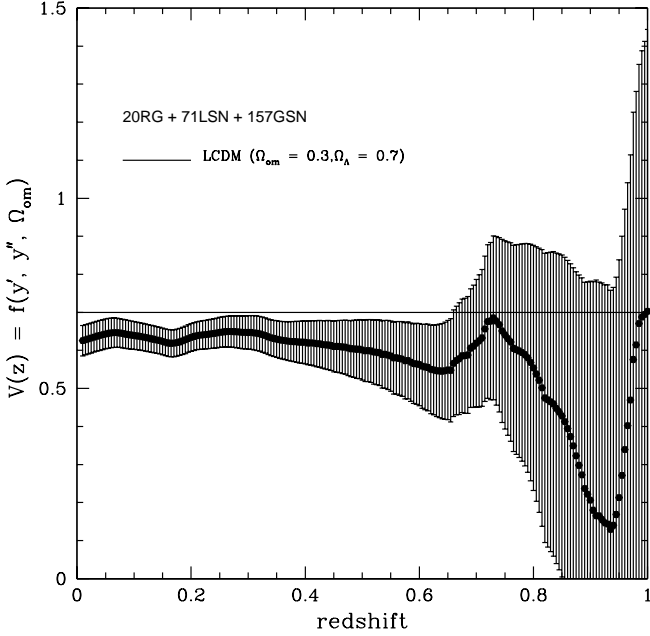


FIG. 17: The potential energy of the dark energy $V(z)$ in units of the critical density today. The zero redshift value is $V_0 = 0.63 \pm 0.05$, whereas the expected value for the standard LCDM model is 0.7.

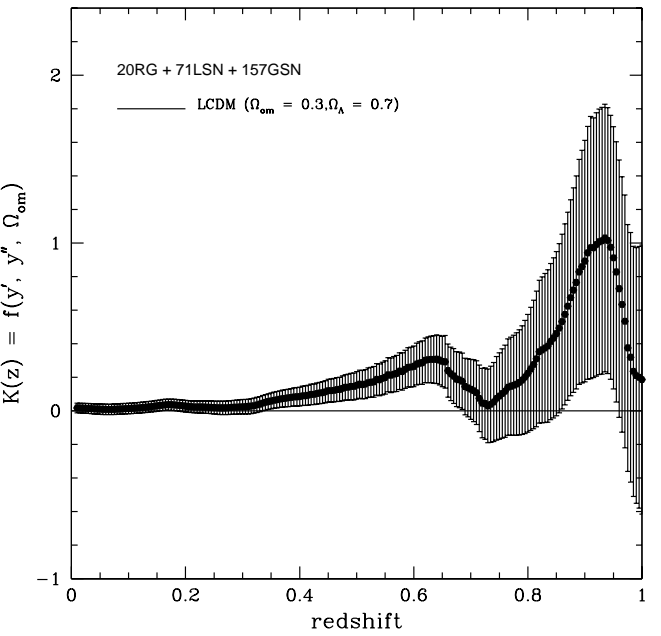


FIG. 19: The kinetic energy of the dark energy $K(z)$ in units of the critical density today. The zero redshift value is $K_0 = 0.02 \pm 0.03$, whereas for the standard LCDM model the expected value is 0.

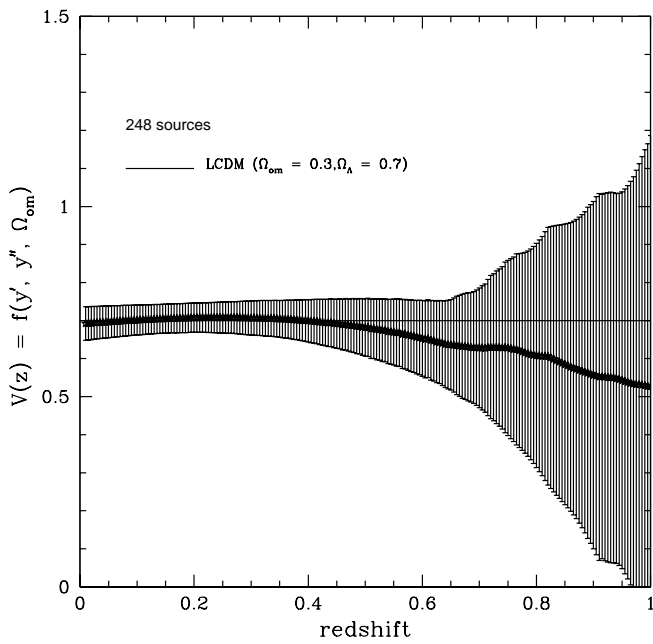


FIG. 18: The values of $V(z)$ for the mock data set. The assumed value of 0.7 is recovered accurately, except for a small bias at the high redshifts.

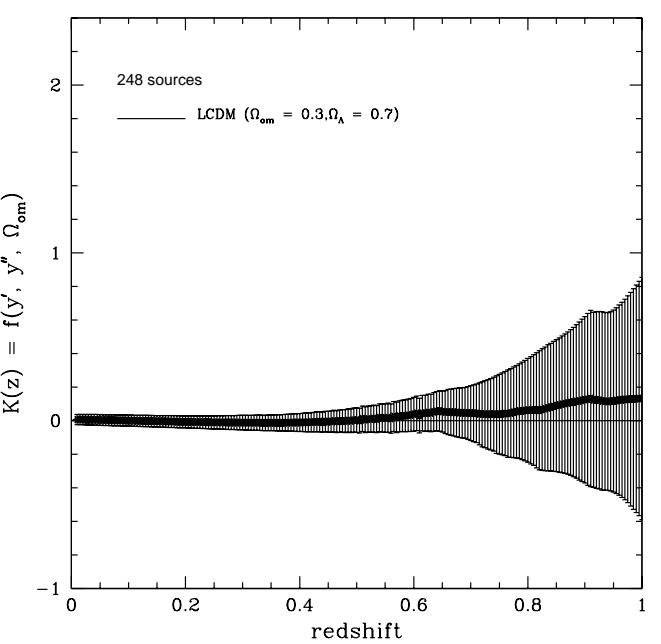


FIG. 20: The values of $K(z)$ for the mock data set. Again, the correct value for the assumed cosmology, $K = 0$, is recovered accurately.

$\Omega_{0m} = 0.3$. The potential energy $V(z)$ is flat, as expected if the dark energy is a cosmological constant, and $K(z)$ is very close to zero, also as expected in a LCDM model. In fact, all of the results obtained here are consistent with expectations in a standard LCDM model since P, f, w, K , and V all remain essentially constant for the redshift range for which the data allow a determination of each quantity. The two modified gravity models shown in Fig. [6] and Fig. [8] do not describe the data as well as the standard LCDM model.

Acknowledgments

It is a pleasure to thank Paul Frampton for helpful discussions related to this work. This work was sup-

ported in part by the U. S. National Science Foundation (NSF) under grants AST-0206002, AST-0507465, and by Penn State University (R. A. D.), and by the NSF grant AST-0407448 and the Ajax Foundation (S. G. D.). We acknowledge the outstanding work and efforts of many observers who obtained the valuable data used in this study.

[1] A. G. Riess, et al., AJ, **116**, 1009 (1998).
 [2] S. Perlmutter et al., ApJ, **517**, 565 (1999).
 [3] J. T. Tonry et al., ApJ, **594**, 1 (2004).
 [4] R. A. Knop et al., ApJ, **598**, 102 (2003).
 [5] Barris, B. J., et al., ApJ, **602**, 571 (2004).
 [6] R. G. Riess, L. Strolger, J. Tonry, S. Casertano, H. G. Ferguson, B. Mobasher, P. Challis, A. V. Filippenko, S. Jha, W. Li, R. Chornock, R. P. Kirshner, B. Leibundgut, M. Dickinson, M. Livio, M. Giavalisco, C. C. Steidel, N. Benitez, and Z. Txvetaanov, ApJ, **607**, 665 (2004).
 [7] P. Astier, et. al, Astron. & Astrophys., submitted, [astro-ph/0510447](http://arxiv.org/abs/astro-ph/0510447).
 [8] D. N. Spergel et al., ApJSupp., **148**, 175 (2003).
 [9] U. Seljak et al., Phys. Rev. D, **71**, 103515 (2005).
 [10] A. G. Sanchez et al., [astro-ph/0507583](http://arxiv.org/abs/astro-ph/0507583).
 [11] E. J. Guerra, R. A. Daly, and L. Wan, ApJ, **544**, 659 (2000).
 [12] R. A. Daly, and E. J. Guerra, AJ, **124**, 1831 (2002).
 [13] S. Podariu, R. A. Daly, M. P. Mory, and B. Ratra, B., ApJ, **584**, 577 (2003).
 [14] R. A. Daly and S. G. Djorgovski, ApJ, **597**, 9 (2003).
 [15] R. A. Daly and S. G. Djorgovski, ApJ, **612**, 652 (2004).
 [16] D. Huterer and M. S. Turner, Phys. Rev. D, **60**, 081301 (1999).
 [17] D. Huterer and M. S. Turner, Phys. Rev. D, **64**, 123527 (2001).
 [18] T. Saini, S. Raychaudhury, V. Sahni, and A. A. Starobinsky, Phys. Rev. Lett., **85**, 1162 (2000).
 [19] M. Tegmark, Phys. Rev. D, **66**, 103507 (2002).
 [20] V. Sahni, T. D. Saini, A. A. Starobinsky, and U. Alam, J. Exp. Theor. Phys. Lett., **77**, 201 (2003).
 [21] D. Huterer and G. Starkman, Phys. Rev. Lett., **90**, 031301 (2003).
 [22] Y. Wang and M. Tegmark, Phys. Rev. Lett., **92**, 241302 (2004).
 [23] Y. Wang and M. Tegmark, Phys. Rev. D., **71**, 103513 (2005).
 [24] J. Simon, L. Verde, and R. Jimenez, Phys. Rev. D **71**, 123001 (2005).
 [25] M. Sahlen, A. R. Liddle, and D. Parkinson, Phys. Rev. D **72**, 083511 (2005).
 [26] M. C. Bento, O. Bertolami, N. M. C. Santos, and A. A. Sen, [astro-ph/0512076](http://arxiv.org/abs/astro-ph/0512076) (2005).
 [27] K. Freese and M. Lewis, Phys. Lett. B., **540**, 1 (2002).
 [28] M. C. Bento, O. Bertolami, and A. A. Sen, Phys. Rev. D., **66**, 043507 (2002).
 [29] A. Y. Kamenshchik, U. Moschella, and V. Pasquier, Phys. Lett. B., **511**, 265 (2001).